

110-43
203386
P. 13

NASA
Technical
Paper
3415

December 1993

A Photogrammetric Solution to a Particular Problem

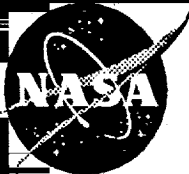
David R. Hedgley, Jr., and
Fanny A. Zuniga

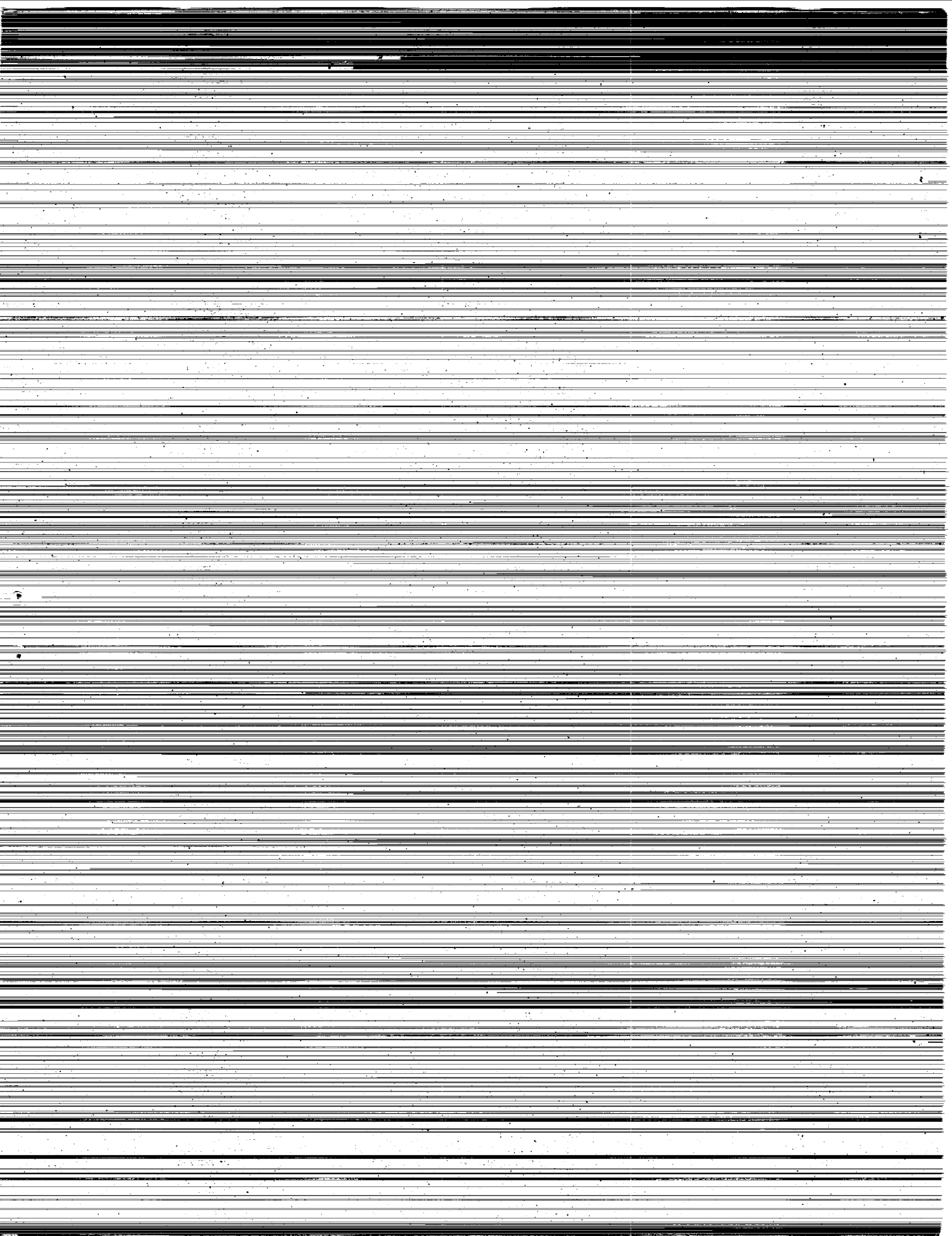
(NASA-TP-3415) A PHOTOGRAMMETRIC
SOLUTION TO A PARTICULAR PROBLEM
(NASA) 13 p

N94-22961

Unclass

H1/43 0203386





National Aeronautics and
Space Administration

Ames Research Center
Dryden Flight Research Facility
P.O. Box 273
Edwards, California 93523-0273

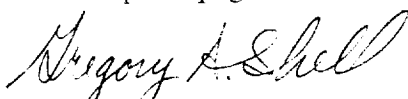


Reply to Attention of: XAR/D-2113/94-18

January 24, 1994

TO: All Holders of NASA TP-3415
FROM: Chief, XAR/Reports and Presentations Branch
SUBJECT: Errata Sheet for NASA TP-3415

Please replace pages 7 and 8 with the enclosed corrected pages.


Gregory A. Shell

Enclosure

**ORIGINAL PAGE IS
OF POOR QUALITY**

**NASA
Technical
Paper
3415**

1993

**A Photogrammetric Solution
to a Particular Problem**

David R. Hedgley, Jr., and
Fanny A. Zuniga
*Dryden Flight Research Facility
Edwards, California*



National Aeronautics and
Space Administration
Office of Management
Scientific and Technical
Information Program



ABSTRACT

A closed-form mathematical solution to the classical photogrammetric problem is presented. Although quite general, the solution is more applicable to problems in which the image-space conjugates are very difficult to match but one of the elements of the pair is not. Additionally, observations are made that should make the solution to the general problem of automatic matching less computationally intensive. This approach was used to analyze flow visualization data for the F-18 High Alpha Research Vehicle. The conditions for this analysis were less than ideal for image-to-object-space transformation.

NOMENCLATURE

Acronyms

HARV	High Alpha Research Vehicle
LEX	leading-edge extension

Symbols

$\hat{a}, A, \hat{b}, B,$ $\hat{c}, C, \hat{d}, f,$ m, s, t, ϵ	} arbitrary constants
---	-----------------------

$\hat{f}, F, g, G,$ $H, I, J, K,$ L, r	} functions
--	-------------

The following symbols are shown in figure 2 (p. 3). Please note that boldfaced coordinates are all located in object space.

u'	x -coordinate with respect to the reference axes (in object space) centered at the primary camera
v'	y -coordinate with respect to the reference axes (in object space) centered at the primary camera
w'	z -coordinate with respect to the reference axes (in object space) centered at the primary camera
X', Y', Z'	x -, y -, and z -coordinates, respectively, of the primary camera with respect to the reference axes
X'', Y'', Z''	x -, y -, and z -coordinates, respectively, of the secondary camera with respect to the reference axes
X_R, Y_R, Z_R	x -, y -, and z -coordinates, respectively, for general rotational formulas (in object space)
x', y'	x - and y -coordinates, respectively, of the photograph with respect to the optical axes of the primary camera (in image space)
x', y', z'	x -, y -, and z -coordinates, respectively, with respect to the optical axes of the primary camera (in object space)
x'', y''	x - and y -coordinates, respectively, of the photograph with respect to the optical axes of the secondary camera (in image space)

x'', y'', z'' x -, y -, and z -coordinates, respectively, with the respect to the optical axes of the secondary camera (in object space)

The following symbols are shown in figure 3 (p. 4):

θ' pitch (elevation) of the primary camera with respect to the reference axes
 θ'' pitch angle of the secondary camera with respect to the reference axes
 ϕ' roll angle of the primary camera with respect to the reference axes
 ϕ'' roll angle of the secondary camera with respect to the reference axes
 ψ' yaw (azimuth) of the primary camera with respect to the reference axes
 ψ'' yaw angle of the secondary camera with respect to the reference axes

INTRODUCTION

In general, the photogrammetric problem may be defined as determining the object-space coordinates of a point, given two photographs of that point taken from two different perspectives. This problem has a very rich history as can be seen from the international interest indicated from a simple literature search.* Moreover, its applications are varied enough to include such fields as oceanography, topography, medicine, astronomy, and aeronautics.

The classical mathematical solution to this problem (ref. 1) is reliable and accurate if all image coordinates given are also accurate. This solution requires that the object be discrete and recognizable in image space and that the two pairs of image coordinates be matched accurately in the two perspectives. In cases, however, where the object is not discrete but rather a continuum of points and the isolated points on the continuum cannot be matched, the classical solution fails to provide accurate object-space coordinates for this particular problem.

This particular problem was encountered in the midst of a flow-visualization experiment on the F-18 High Alpha Research Vehicle (HARV) at the NASA Dryden Flight Research Facility. The overall objective of this experiment was to study the vortical behavior and structure of the flow at high angles of attack for an F-18 aircraft using in-flight flow visualization (ref. 2). In an effort to provide quantitative flight data and to allow for calibration of computational fluid dynamic codes, it became important to accurately map out the LEX vortex core path using the existing flow-visualization data. The flow visualization data were acquired by two cameras. The primary camera was located at the right wingtip, and the secondary camera was located on the right vertical stabilizer (fig. 1). Because of the inability to isolate any single point in the continuum of points identified in the perspectives, it was impossible to precisely match a pair of image-space coordinates from the primary camera view (x' , y') with a pair of coordinates from the secondary camera view (x'' , y'') (fig. 2). Since x'' of the second perspective changed minimally along the continuum of points identified, it was possible to transform discrete points from image space to object space using only three image-space coordinates (x' , y') and x'' , or even (x' , y') and y'' . The motivation for this paper rests in finding a closed-form stable solution to this classical problem that uses three image-space coordinates and, therefore, is not perturbed unduly by uncertain data.

The author gratefully acknowledges the contributions of Howard R. Trent and Rodney K. Bogue of NASA Dryden and Denis Elliott of the Joint Propulsion Laboratory, California Institute of Technology, Pasadena, California.

* For example, NASA RECON yielded 3483 possible sources of information.

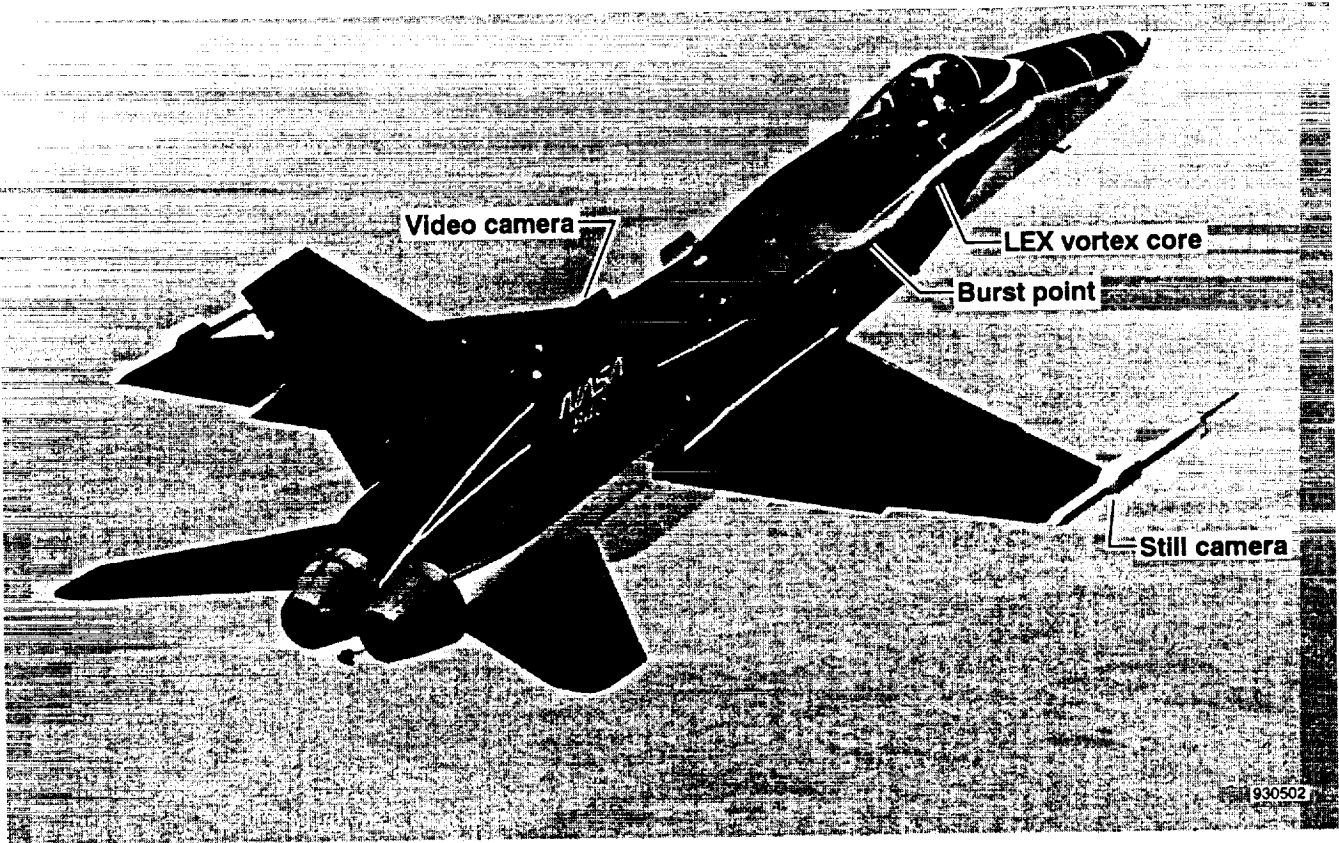


Figure 1. The F-18 HARV with smoke visualizing the LEX vortex core and burst point.

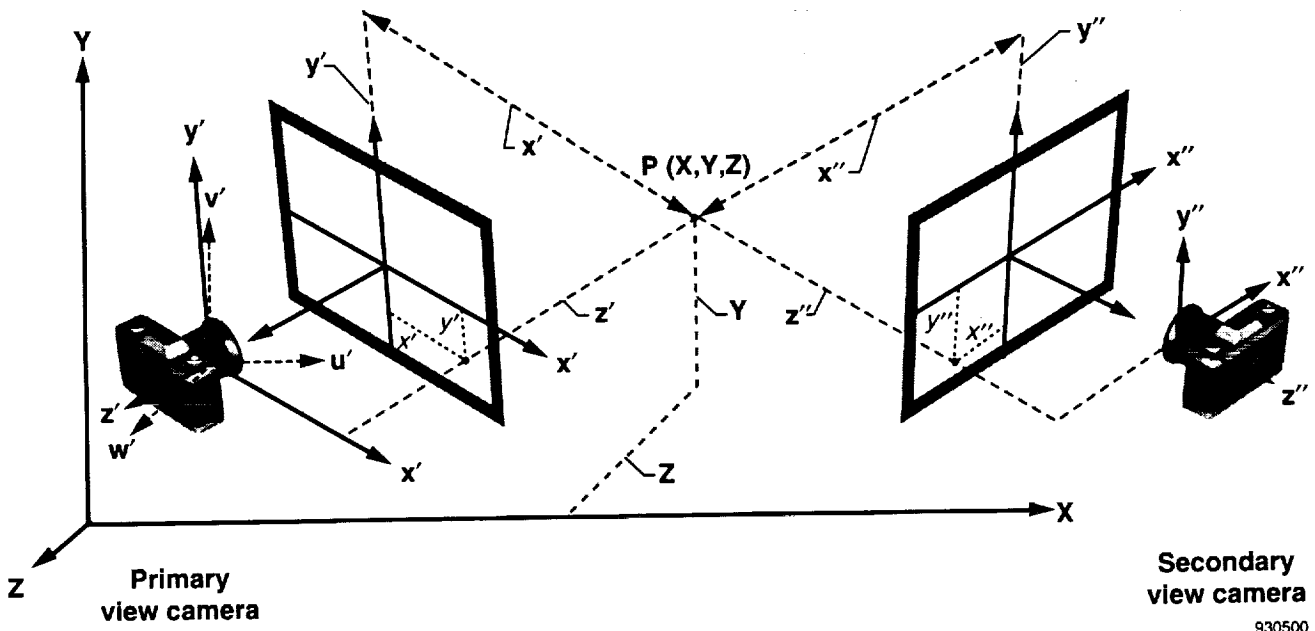


Figure 2. Reality and photography.

ANALYSIS

The following discussion will first address the definition of both the axes system and Eulerian angles convention. Second, a general solution to the photogrammetric problem will be formulated.

The reference axes system is a right-handed convention as defined in figures 2 and 3. The arrows denote the positive directions of the axes, while the positive angular rotations are counterclockwise in the plane of definition.

Let (X, Y, Z) be the coordinates of an arbitrary point (P in fig. 2) in three-dimensional space. Then the following equations given by

$$X_R = X \cos \phi \cos \psi + Y \sin \phi - Z \cos \phi \sin \psi \quad (1)$$

$$Y_R = X (\sin \psi \sin \theta - \sin \phi \cos \theta \cos \psi) + Y \cos \phi \cos \theta + Z (\sin \theta \cos \psi + \sin \phi \cos \theta \sin \psi) \quad (2)$$

$$Z_R = X (\cos \theta \sin \psi + \sin \phi \sin \theta \cos \psi) - Y \cos \phi \sin \theta + Z (\cos \theta \cos \psi - \sin \phi \sin \theta \sin \psi) \quad (3)$$

are rotational equations where (X_R, Y_R, Z_R) represents the point (X, Y, Z) in the orthogonally rotated axes system (ψ, ϕ, θ) . These formulas will be the basic equations used in the derivation. Note that given the axes convention and the physical restraint of the problem, $Z < 0$ implying that $|Z| = -Z$.

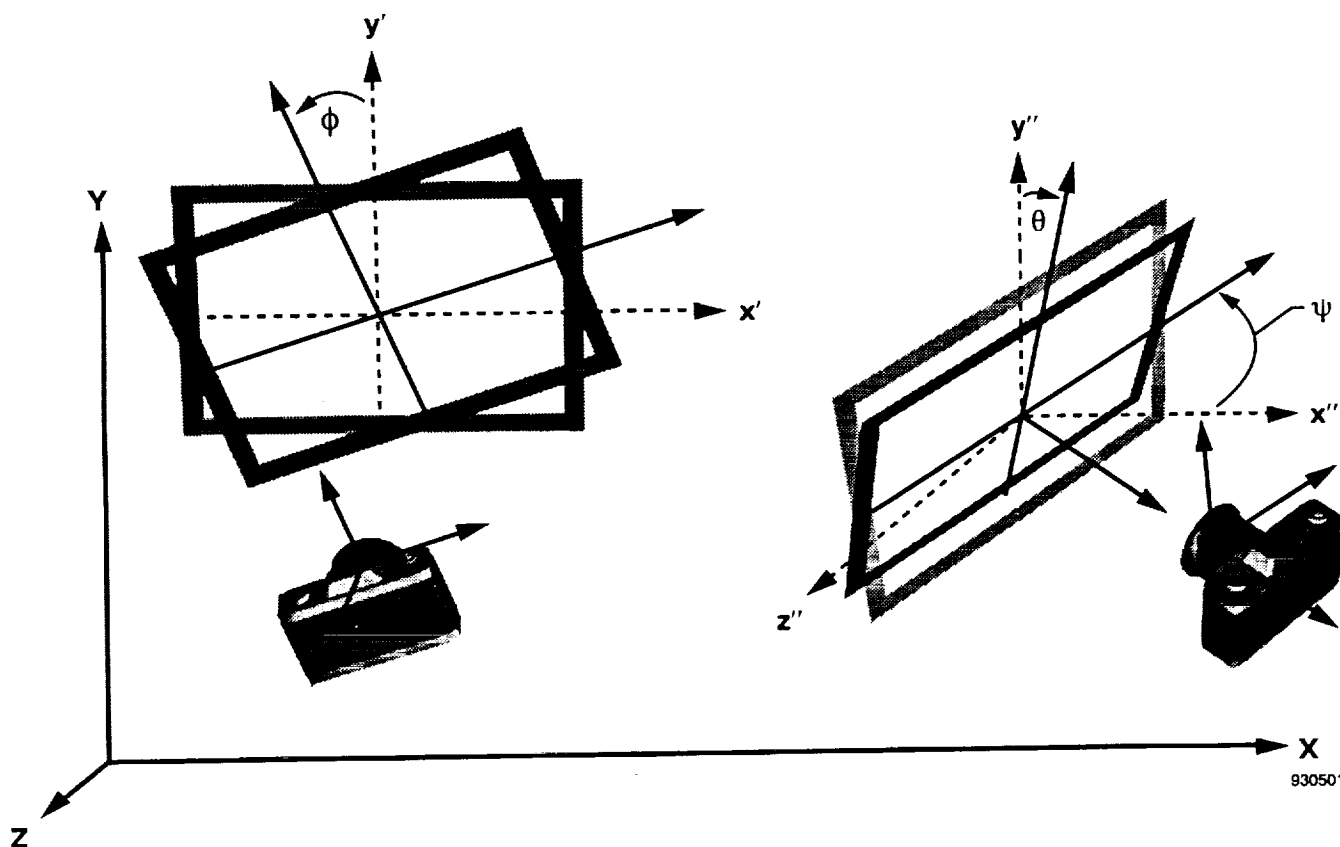


Figure 3. Eulerian angles.

From elementary optics (ref. 1) $\frac{aX'}{|Z'|} = x'$, where $a = f \times m$, f is the focal length of the camera, and m is the magnification of the film (fig. 2). Clearly, $X' = -\frac{x'Z'}{a}$, and similarly $Y' = -\frac{y'Z'}{a}$. From equation (1),

$$-\frac{x'Z'}{a} = u' \cos \phi' \cos \psi' + v' \sin \phi' - w' \cos \phi' \sin \psi' \quad (4)$$

Thus

$$u' = F(v', w', Z') \quad (5)$$

From equation (2),

$$-\frac{y'Z'}{a} = u' (\sin \psi' \sin \theta' - \sin \phi' \cos \theta' \cos \psi') + v' (\cos \phi' \cos \theta') + w' (\sin \theta' \cos \psi' + \sin \phi' \cos \theta' \sin \psi') \quad (6)$$

Upon substituting equation (5) and simplifying, we have

$$v' = G(w', Z') \quad (7)$$

Substituting equation (7) in equation (5), we have

$$u' = H(w', Z') \quad (8)$$

From equation (3),

$$Z' = u' (\cos \theta' \sin \psi' + \sin \theta' \cos \psi') - v' \cos \phi' \sin \theta' + w' (\cos \theta' \cos \psi' - \sin \phi' \sin \theta' \sin \psi') \quad (9)$$

Substituting equations (8) and (7), we have

$$Z' = H(Z', w') (\cos \theta' \sin \psi' + \sin \phi' \sin \theta' \cos \psi') - G(w', Z') \cos \phi' \sin \theta' + w' (\cos \theta' \cos \psi' - \sin \phi' \sin \theta' \sin \psi') \quad (10)$$

Thus

$$Z' = I(w') \quad (11)$$

Substituting equation (11) in equations (8) and (7), we have

$$u' = J(w'), v' = K(w') \quad (12)$$

Let

$$\Delta X = X' - X''$$

$$\Delta Y = Y' - Y''$$

$$\Delta Z = Z' - Z''$$

Then the depth with respect to the secondary camera's axes system can be written as

$$Z'' = (u' + \Delta X) [\cos \theta'' \sin \psi'' + \sin \phi'' \sin \theta'' \cos \psi''] - (v' + \Delta Y) [\cos \phi'' \sin \theta''] + (w' + \Delta Z) [\cos \theta'' \cos \psi'' - \sin \phi'' \sin \theta'' \sin \psi''] \quad (13)$$

Substituting equation (12), we have

$$Z'' = L(w') \quad (14)$$

Again from equations (14), (1), and (12),

$$\mathbf{x}'' = -\frac{x'' \mathbf{z}''}{a} = -\frac{x'' L(\mathbf{w}')}{a} = (J(\mathbf{w}') + \Delta X) \cos \phi'' \cos \psi'' + (K(\mathbf{w}') + \Delta Y) \sin \phi'' - (\mathbf{w}' + \Delta Z) (\cos \phi'' \sin \psi'') \quad (15)$$

This is an equation linear in \mathbf{w}' ; thus, the solution is

$$\begin{aligned} \mathbf{w}' &= s \\ \mathbf{u}' &= J(s) \\ \mathbf{v}' &= K(s) \end{aligned} \quad (16)$$

and represents the solution with respect to the reference axes system centered at the center of the principal axes of the primary camera.

A similar result is possible if only y'' is known using equation (2). In particular,

$$\begin{aligned} \mathbf{y}'' = -\frac{y'' L(\mathbf{w}')}{a} &= (J(\mathbf{w}') + \Delta X) [\sin \psi'' \sin \theta'' - \sin \phi'' \cos \theta'' \cos \psi''] \\ &+ (K(\mathbf{w}') + \Delta Y) [\cos \phi'' \cos \theta''] \\ &+ (\mathbf{w}' + \Delta Z) [\sin \theta'' \cos \psi'' + \sin \phi'' \cos \theta'' \sin \psi''] \end{aligned} \quad (17)$$

Equations (15) and (17) can be rewritten as follows:

$$\mathbf{w}' = g(x''); \quad \mathbf{w}' = r(y'') \quad (18)$$

Thus $g(x'') = r(y'')$, which simplifies to an equation of the form

$$Ax'' + By'' + C = 0 \quad (19)$$

This equation represents the line in the projection plane of the secondary image that contains the conjugate (x'', y'') (ref. 3). This observation is important because it restricts the area of search required as it relates to the automatic matching problem (ref. 3). Moreover, the following analysis may be employed to enhance the efficiency of the search.

Equation (18) may be represented as

$$g(x'') = \mathbf{w}' = \frac{\hat{a}x'' + \hat{b}}{\hat{c}x'' + \hat{d}} \quad (20)$$

In addition, if x_0'' is the singularity of equation (20) (i.e., $x_0'' = -\hat{d}/\hat{c}$) and $-t < x_0'' < t$ where $2t$ is the width of the photograph, then for $\varepsilon > 0$

$$\hat{f}(\varepsilon) = \frac{[\hat{a}(x_0'' + \varepsilon) + \hat{b}][\hat{a}(x_0'' - \varepsilon) + \hat{b}]}{[\hat{c}(x_0'' + \varepsilon) + \hat{d}][\hat{c}(x_0'' - \varepsilon) + \hat{d}]} = \frac{(\hat{a}x_0'' + \hat{b} + \hat{a}\varepsilon)(\hat{a}x_0'' + \hat{b} - \hat{a}\varepsilon)}{(-\hat{c}\varepsilon)(\hat{c}\varepsilon)} \quad (21)$$

Thus $\hat{f}(\varepsilon) < 0$, if $\varepsilon < \left| \frac{\hat{a}x_0'' + \hat{b}}{\hat{a}} \right|$

Then, given ε to be arbitrarily small, either $g(x_0'' + \varepsilon) < 0$ or $g(x_0'' - \varepsilon) < 0$ but not both. And considering the axes convention, $g(x) > 0$ is nonsensical. Therefore, the interval of search lies in $[-t, x_0'' - \varepsilon]$ or $[x_0'' + \varepsilon, t]$. In addition, if this interval is substituted in equation (19) and subsequent restrictions are imposed on y'' because of the photograph's vertical dimension, an even smaller interval may result. Hence the additional restraint on the search

imposed by this interval could be very useful provided nothing else is known about the three-dimensional scene. If the approximate depth (z) is known, then equation (20) may be solved for x'' in which case the above reasoning becomes unnecessary.

APPLICATION

As mentioned earlier the formulation just described was developed during an F-18 experiment at NASA Dryden in an effort to accurately map the leading-edge extension (LEX) vortex core path from in-flight off-surface flow visualization. A smoke-generator system that injected smoke into the flow field was used on the F-18 HARV (ref. 4) to visualize the LEX vortex core in flight at high angles of attack (fig. 1). From still and video images recorded on board, image-space coordinates corresponding to the path of the vortex core from two opposing views were tabulated and processed to output object-space coordinates in an aircraft coordinate system.

Figures 4 and 5 show the right-wingtip primary camera view and the right-vertical-tail secondary camera view of the LEX vortex core along with the vortex core burst point. Shown also on these figures are the image-space coordinates (x', y') and (x'', y'') as projected on the center of the photos. Image-space coordinates from the primary view, (x', y') , were matched with x'' of the secondary view. Since x'' of the secondary view typically changed by less than half an inch from the beginning to the burst point of the vortex core, the uncertainty in x'' was kept to within ± 0.0625 in. In addition, taking into account small displacements in the camera position and rotation caused by the aeroelasticity of the F-18 HARV, the accuracy of the solution sets was limited to 4 in. or 2 percent of the actual aircraft length. This uncertainty slightly increased to 6 in. with increasing angle of attack since the width of the vortex core increased, thus limiting the ability of the smoke to precisely define the vortex core.

The object-space coordinates of the LEX vortex core path in an aircraft coordinate system are presented in figure 6 for angles of attack of 15.0° , 19.6° , 25.0° , 29.8° , and 35.0° . The data used for these results were taken at steady-state flight conditions where angle of sideslip was kept to within $\pm 0.5^\circ$. No results are shown for angles of attack greater than 35° because steady-state conditions were no longer obtainable at these angles of attack.

As can be noted from figure 6, with increasing angle of attack, the vortex core path is seen to rise higher off the surface and move slightly inboard. These trends are consistent with the flow-visualization results reported in reference 2. Comparisons of the solution sets, however, could not be made quantitatively because this is the only quantitative solution set of the LEX vortex core path for an F-18 aircraft at high angles of attack.

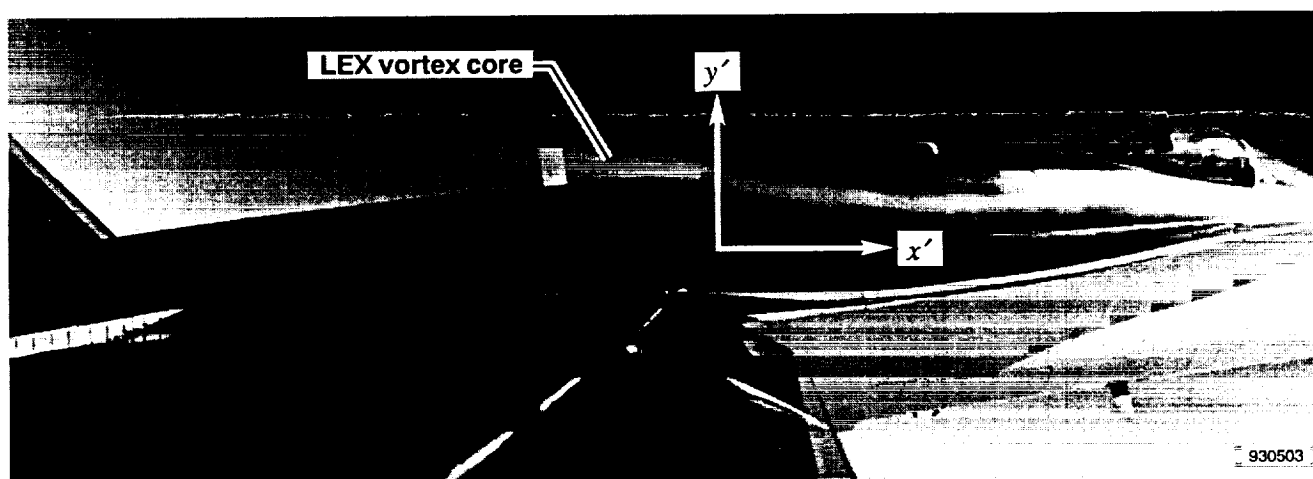


Figure 4. Right-wingtip camera view of the LEX vortex core.

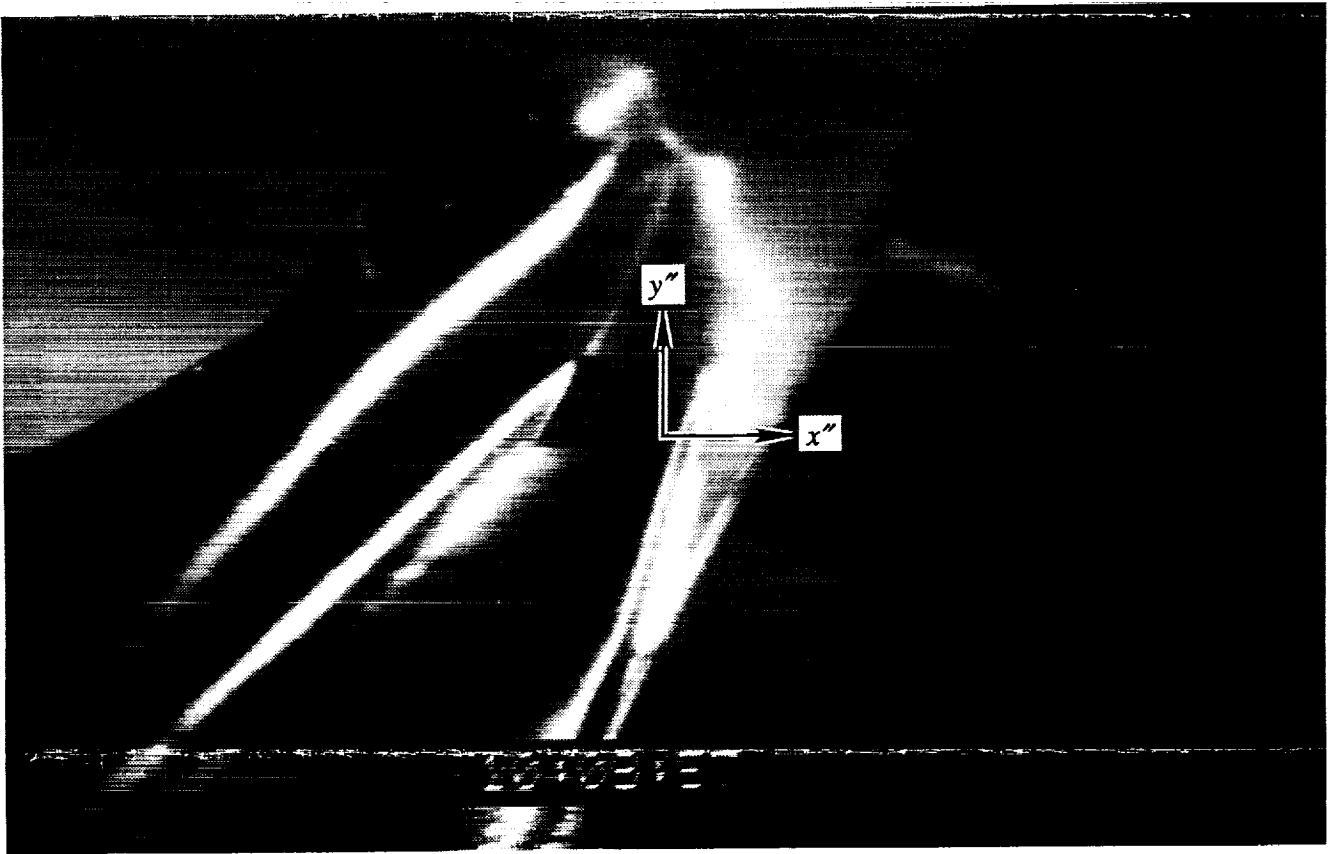
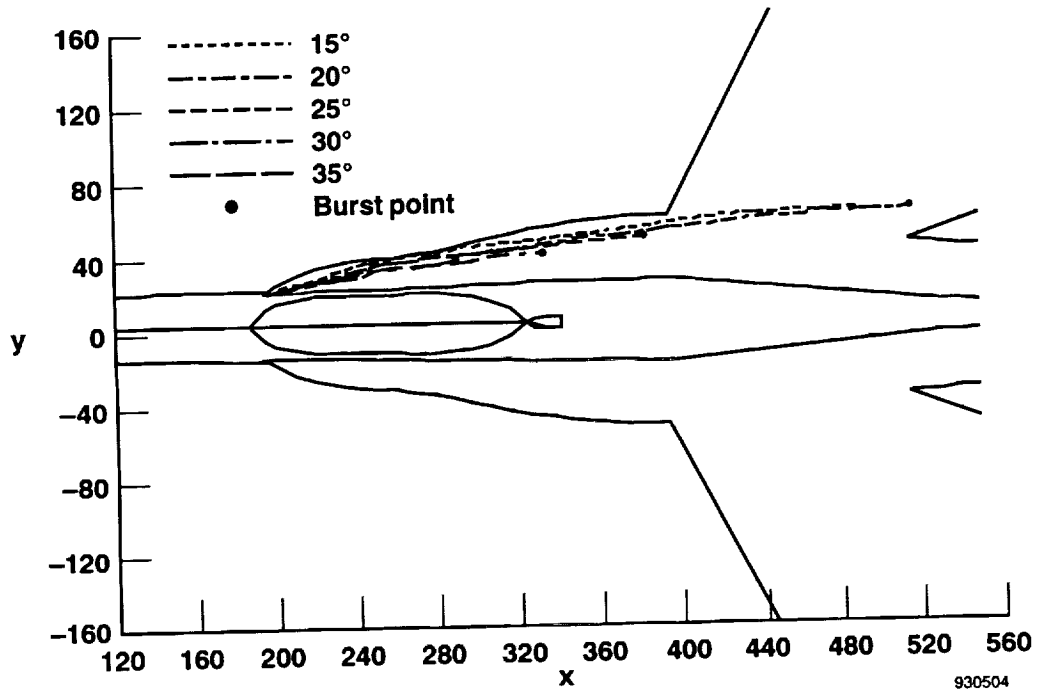
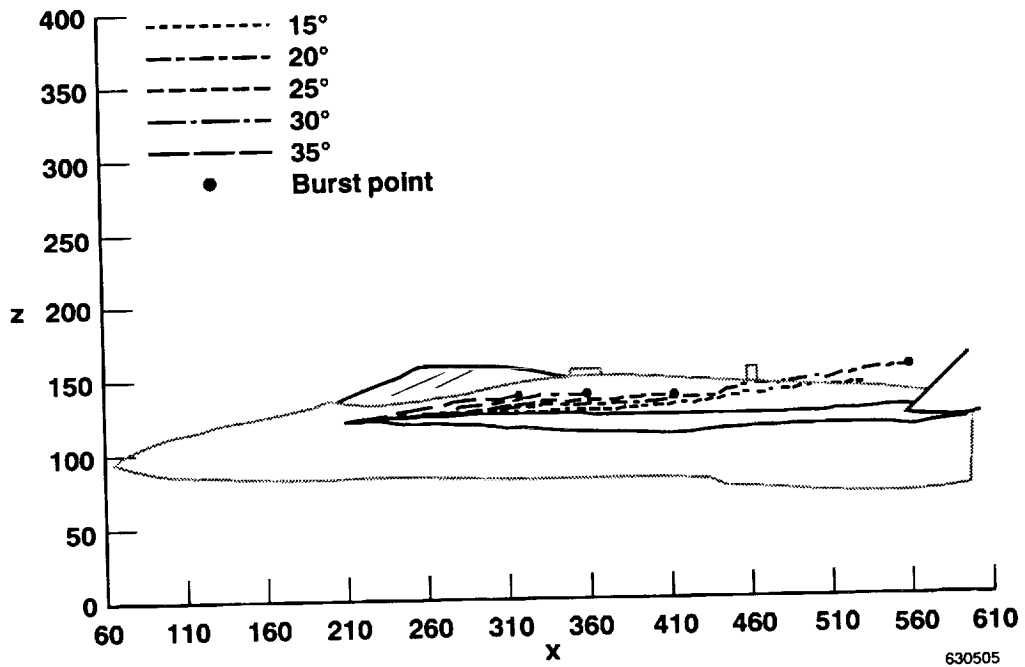


Figure 5. Right-vertical-tail camera view of the LEX vortex core.



(a) Top view.



(b) Side view.

Figure 6. Angle-of-attack effects on the right-wing LEX vortex core and burst point.

Only one time point of data was used to reconstruct each of the vortex core paths shown in figure 6. Because of the dynamic motion of the vortex core at these high angles of attack even during steady-state conditions, averaged results of the vortex path over several time points would be preferable in giving better solutions of the vortex path. The improvement of the image-processing techniques currently being used is underway, which will allow for better results.

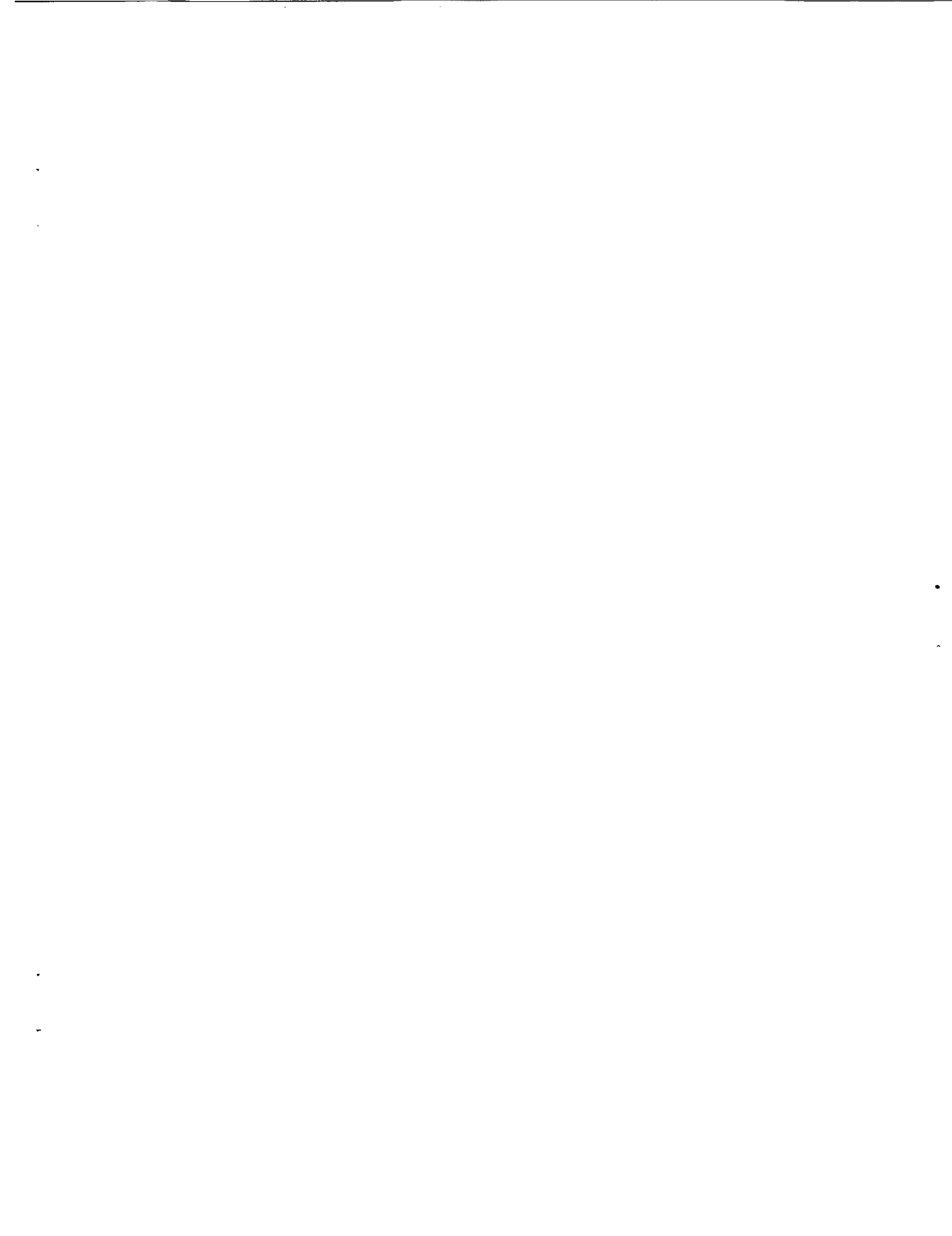
CONCLUSION

A closed-form mathematical solution to the classical photogrammetric problem has been presented. Additionally, the observations made here should make the solution to the automatic matching problem less computationally intensive.

This approach was used to analyze the F-18 High Alpha Research Vehicle flow-visualization data. The technique proved successful in reconstructing the vortex core paths from image space to object space where the accuracy of the solution sets was stated within 4 to 6 in. Comparisons of the solution sets, however, could not be made quantitatively because this is the only quantitative solution set of the leading-edge extension vortex core path for an F-18 aircraft at high angles of attack.

REFERENCES

1. Moffitt, Francis H., *Photogrammetry*, Harper and Row Publishers, New York, New York, 1980, pp. 442-448.
2. Del Frate, John H. and Fanny A. Zuniga, "In-Flight Flow Field Analysis on the NASA F-18 High Alpha Research Vehicle With Comparisons to Ground Facility Data," AIAA 90-0231, Jan. 1990.
3. Horn, Berthold, *Robot Vision*, MIT Press, Boston, MA, 1986, pp. 308-322.
4. Richwine, David M. and Robert E. Curry, *A Smoke Generator for Aerodynamic Flight Research*, NASA TM-4137, 1989.



REPORT DOCUMENTATION PAGE

Form Approved
OMB No. 0704-0188

Public reporting burden for this collection of information is estimated to average 1 hour per response, including the time for reviewing instructions, searching existing data sources, gathering and maintaining the data needed, and completing and reviewing the collection of information. Send comments regarding this burden estimate or any other aspect of this collection of information, including suggestions for reducing this burden, to Washington Headquarters Services, Directorate for Information Operations and Reports, 1215 Jefferson Davis Highway, Suite 1204, Arlington, VA 22202-4302, and to the Office of Management and Budget, Paperwork Reduction Project (0704-0188), Washington, DC 20503.

1. AGENCY USE ONLY (Leave blank)	2. REPORT DATE December 1993	3. REPORT TYPE AND DATES COVERED Technical Paper	
4. TITLE AND SUBTITLE A Photogrammetric Solution to a Particular Problem		5. FUNDING NUMBERS WU 505-68-71	
6. AUTHOR(S) David R. Hedgley, Jr., and Fanny A. Zuniga		8. PERFORMING ORGANIZATION REPORT NUMBER H-1888	
7. PERFORMING ORGANIZATION NAME(S) AND ADDRESS(ES) NASA Dryden Flight Research Facility P.O. Box 273 Edwards, California 93523-0273		10. SPONSORING/MONITORING AGENCY REPORT NUMBER NASA TP-3415	
9. SPONSORING/MONITORING AGENCY NAME(S) AND ADDRESS(ES) National Aeronautics and Space Administration Washington, DC 20546-0001		11. SUPPLEMENTARY NOTES	
12a. DISTRIBUTION/AVAILABILITY STATEMENT Unclassified—Unlimited Subject Category 43		12b. DISTRIBUTION CODE	
13. ABSTRACT (Maximum 200 words) <p style="text-align: center;">A closed-form mathematical solution to the classical photogrammetric problem is presented. Although quite general, the solution is more applicable to problems in which the image-space conjugates are very difficult to match but one of the elements of the pair is not. Additionally, observations are made that should make the solution to the general problem of automatic matching less computationally intensive. This approach was used to analyze flow visualization data for the F-18 High Alpha Research Vehicle. The conditions for this analysis were less than ideal for image-to-object-space transformation.</p>			
14. SUBJECT TERMS F-18 aircraft, Flow visualization, Photogrammetry		15. NUMBER OF PAGES 13	16. PRICE CODE AO3
17. SECURITY CLASSIFICATION OF REPORT Unclassified	18. SECURITY CLASSIFICATION OF THIS PAGE Unclassified	19. SECURITY CLASSIFICATION OF ABSTRACT Unclassified	20. LIMITATION OF ABSTRACT Unlimited